

Wind and Topographic Effects on the Labrador Current at Carson Canyon

E. DOUGLAS KINSELLA,¹ ALEX E. HAY, AND WARREN W. DENNER²

Department of Physics and Newfoundland Institute for Cold Ocean Science, Memorial University of Newfoundland, St. John's

We present results from an experimental investigation of the interaction between a shelf break jet and a submarine canyon and of the response of this system to a single upwelling favorable wind event. The field site was Carson Canyon, located at the edge of the Grand Bank of Newfoundland. The shelf break jet is the Labrador Current. The time-averaged current measurements indicate that the interaction between the Labrador Current and the canyon topography is nonlinear and that the mean current crosses isobaths to flow into the canyon on the upstream side but is steered off shelf on the downstream side. The mean flow vorticity balance in the near field and far field is examined, using a two-layer model with the lower layer at rest. In the far field we obtain an interesting result which suggests that the cross-stream shear in combination with bottom friction can drive a significant on-shelf flow. This flow is equivalent to a volume transport of about $60 \text{ m}^3 \text{ s}^{-1}$ per 100 m of along-shelf distance, which is comparable to typical wind-driven Ekman transports on and off continental shelves and which appears to have important implications for the on-off-shelf transport of icebergs in the Grand Banks region. In the near field the Rossby number is of order unity and bottom friction is less important. Many of the observed flow properties can be explained qualitatively in terms of an upstream inertial boundary layer and potential vorticity conservation. The time-dependent response to upwelling favorable winds was registered by current meters in the canyon and at the shelf break at the canyon perimeter. These observations indicate an amplified upwelling response at the shelf break and vertical ascent rates within the canyon of about 0.7 cm s^{-1} .

1. INTRODUCTION

Although submarine canyons are characteristic of the shelf break environment, there have been few studies of circulation within and in the immediate vicinity of these pronounced topographic features. The literature has been reviewed by *Huthnance* [1981] and previously by *Inman et al.* [1976]. *Shepard et al.* [1979] summarize current measurements from a variety of canyons. *Hotchkiss and Wunsch* [1982] discuss a rather more detailed set of observations from Hudson Canyon and, in particular, the association of strong currents with storms, internal waves, and internal tides. In general, significant along-canyon motions can be expected, with the consequence that in many of the studies to date [*Coachman and Barnes*, 1962; *Shaffer*, 1976; *Mayer et al.*, 1981, 1982; *Freeland and Denman*, 1982], it has been found that canyons are sites of preferential exchange between the shelf and slope. Such exchange may have important consequences for biological productivity and residence times on the adjacent shelf.

Carson Canyon is the northernmost of a series of canyons which indent the shelf and slope along the southeastern edge of the Grand Bank (Figure 1). The dominant feature of the physical oceanography of this region is the Labrador Current, which flows from northeast to southwest approximately parallel to the 200-m isobath (Figure 1a). Typically, the Labrador Current is confined to the upper 200–300 m of the water column and has a width of about 50 km and a mean speed at its core of about 50 cm s^{-1} . The reader is referred to the article by *Petrie and Anderson* [1983] for a summary of the

properties of the Labrador Current in the Grand Banks region and a review of the associated literature.

The physical situation therefore is one in which a baroclinic jet trapped at the shelf break encounters the abrupt canyon topography. The problem is to determine how this interaction affects the dynamics of the jet and the residual circulation in the canyon. The coupling of the jet to the shelf-slope topography upstream and downstream of the canyon is part of this problem. The effects of time-dependent winds on the coupled canyon-current system are also of interest, particularly in view of the possible consequences for wind-induced upwelling and exchange at the shelf break [*Hay and Kinsella*, 1986].

The purpose of this paper is to present observations obtained in the vicinity of Carson Canyon to provide a basis for discussion of the problems mentioned above. The paper is organized as follows: Brief descriptions of the study area and methodology are given in section 2. The experimental results are presented in section 3. The implications and physical interpretation of these results are discussed in section 4.

2. STUDY AREA AND METHODS

The bathymetry in the vicinity of Carson Canyon is shown in Figure 1b. The shelf break is in the vicinity of the 100-m isobath. The canyon itself is approximately 10 km wide and intrudes about 15 km into the shelf. A small secondary canyon is present on the northeastern side.

Two experiments were undertaken, one in June 1980 from MV *Gadus Atlantica* and the second in June 1981 from MV *Pandora II*. Each cruise involved conductivity, temperature, and depth (CTD) and moored current meter measurements. A Guildline Series 8750 CTD system was used in 1980, and a Neil Brown Instrument Systems Mark III CTD was used in 1981. Aanderaa RCM4 current meters with temperature sensors were used in 1980 and with temperature and conductivity sensors in 1981. Salinities were calculated using the *Bennett* [1976] formula. Time series of wind speed and direction and tidal height were available from the offshore drilling rigs at

¹Now at Edgerton, Germeshausen, and Grier, Incorporated, Waltham, Massachusetts.

²Now at Science Applications International Corporation, Monterey, California.

Copyright 1987 by the American Geophysical Union.

Paper number 7C0413.
0148-0227/87/007C-0413\$05.00

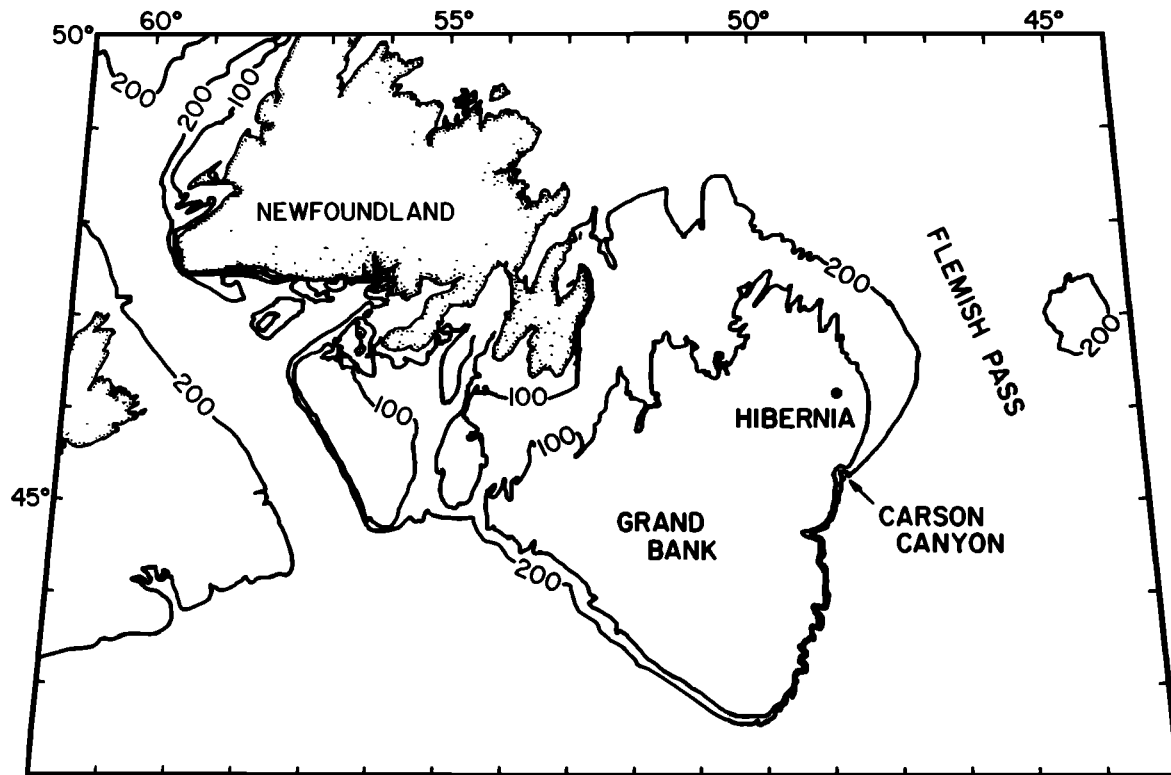


Fig. 1a. Location map showing Newfoundland, the Grand Bank, and Carson Canyon.

Hibernia 85 km due north of Carson Canyon (Figure 1a). Surface pressure charts were obtained from the Atmospheric Environment Service, Canada. The current meter data were despiked and then low-pass filtered, using a moving average filter [Godin, 1972, pp. 60–69] with a 1.4-hour cutoff to remove high-frequency variations and with a 33.2-hour cutoff to remove the tides.

3. RESULTS

3.1. June 1980

CTD data were collected during the period from June 1 to 6, 1980, at the stations shown in Figure 1b. Temperature and salinity sections extending seaward from the shelf are presented in Figure 2. Three pairs of sections are shown: one on the northeastern side of the canyon (Figures 2a and 2b), one along the canyon axis (Figures 2c and 2d), and one on the southwestern side (Figures 2e and 2f). These sections may be located with respect to the canyon (Figure 1b) by referring to the CTD station numbers along the bottom of each panel in Figure 2. Note that stations 39 and 40 are common to both the central axis and southwestern sections. Because density is controlled almost entirely by salinity at these low temperatures ($<4^{\circ}\text{C}$), the corresponding σ_t sections are not shown.

The most prominent feature in these data is Labrador Current water, which can be recognized as the body of low-temperature water ($<1^{\circ}\text{C}$) perched at the edge of the shelf in the 50- to 200-m depth range. The isohalines within and immediately below this cold water slope downward toward the shelf and indicate the presence of the Labrador Current in the upper 200 to 300 m of the water column, trapped against the

shelf break and slope. The direction of the flow is southwestward: that is, with shallow water to the right.

A core of very cold water ($\leq -1^{\circ}\text{C}$) is present in all sections in the 50- to 90-m depth range. In the upstream (northeastern) and downstream (southwestern) sections (Figures 2a and 2e), the cold core is located over and seaward of the shelf break. In the central axis section (Figure 2c) this very cold water is slightly deeper, and in fact, two cold cores are present, one being located over the shelf break at the head of the Canyon, the other farther seaward.

Two current meter moorings, each supporting a single instrument, were deployed slightly seaward of the shelf break upstream and downstream of the Canyon in June 1980 for 6.5 and 5 days, respectively. The upstream instrument was located 10 m above bottom at 164-m depth; the downstream instrument was located 8 m above bottom at 120-m depth. The mean velocity vectors constructed from the average of the 33.2-hour cutoff low-pass filtered records are shown in Figure 1b. The magnitudes of both vectors are similar, being 20 and 17 cm s^{-1} for the upstream and downstream instruments, respectively. The flow at each instrument is nearly parallel to the local isobaths, although a slight shelfward deflection is present (about 13° and 14° at the upstream and downstream instruments, respectively). This is opposite to that expected from Ekman veering in the bottom boundary layer.

The temperature data and the along-isobath (J , positive along 190° T) and cross-isobath (I , positive along 280° T) current components from the downstream meter are presented in Figure 3, together with the tidal elevation and wind speed and direction measured at Hibernia (Figure 1a). These data are presented primarily for comparison with the 1981 data set,

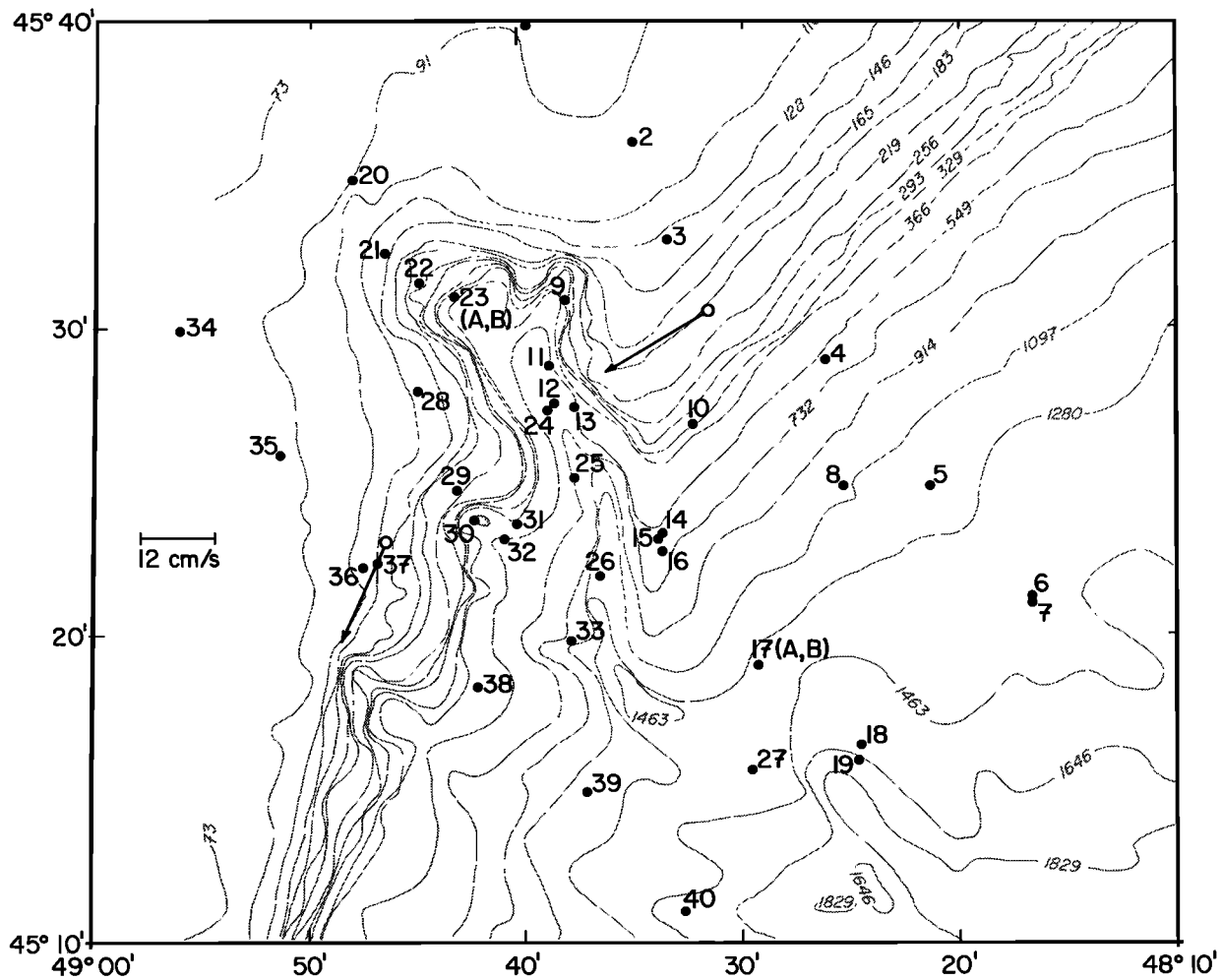


Fig. 1b. Detailed bathymetry of Carson Canyon, 1980 CTD station locations, and the 1980 current meter positions and mean current vectors. Depths in meters.

which is discussed in section 3.2. The temperature is tidally modulated. Maximum temperatures coincide with measured high water and occur after periods of maximum on-shelf flow (positive I) during flood. Correspondingly, temperature minima coincide with low water, occurring after maximum off-shelf flow (negative I) during ebb. The along-isobath component J is also tidally modulated, but never zero or negative, indicating that the tide was not sufficiently strong to cause flow reversal. The wind speeds are less than 16 m s^{-1} and slowly varying (in the sense defined in section 3.2).

3.2. June 1981

The location of the CTD stations and three current meter moorings for the 1981 experiment are shown in Figure 4. Axial sections of temperature and salinity constructed from CTD profiles collected on June 11 are presented in Figure 5 and may be compared with the sections from the previous year (Figure 2). Labrador Current water ($< 1^\circ\text{C}$) at and seaward of the shelf break is again evident, as is the cold-water core ($< -1^\circ\text{C}$). Unlike the previous year, there is no indication that the cold core splits over the canyon. Also unlike the previous year, and this is the most important difference as far

as the present discussion is concerned, the isohalines and isotherms at and below 120-m depth are nearly horizontal in the zone 8–12 km seaward of the shelf break. Unfortunately, we were unable to occupy this axial section prior to June 11. However, a CTD profile collected 5 days previously at station 2 demonstrates that warmer, more saline water had been displaced upward in this region at some time during the period June 6–11 [Kinsella, 1984].

Current meter moorings were deployed upstream, downstream, and on the canyon axis, as shown in Figure 4. The upstream and downstream moorings were both located slightly to seaward of the shelf break, about 6 km from the central axis mooring, and each supported a single instrument at 144-m and 145-m depth, respectively, at a height of 10 m above bottom. A shallow instrument at 168-m depth and a second instrument 10 m above bottom at 703-m depth were mounted on the central axis mooring. The 1.4-hour cutoff low-pass filtered temperature records from the three shallow instruments are presented in Figure 6, together with the measured tidal elevation at Hibernia. The tidal amplitudes are similar to those in the previous year (Figure 3d), and the temperature records from the central axis and upstream

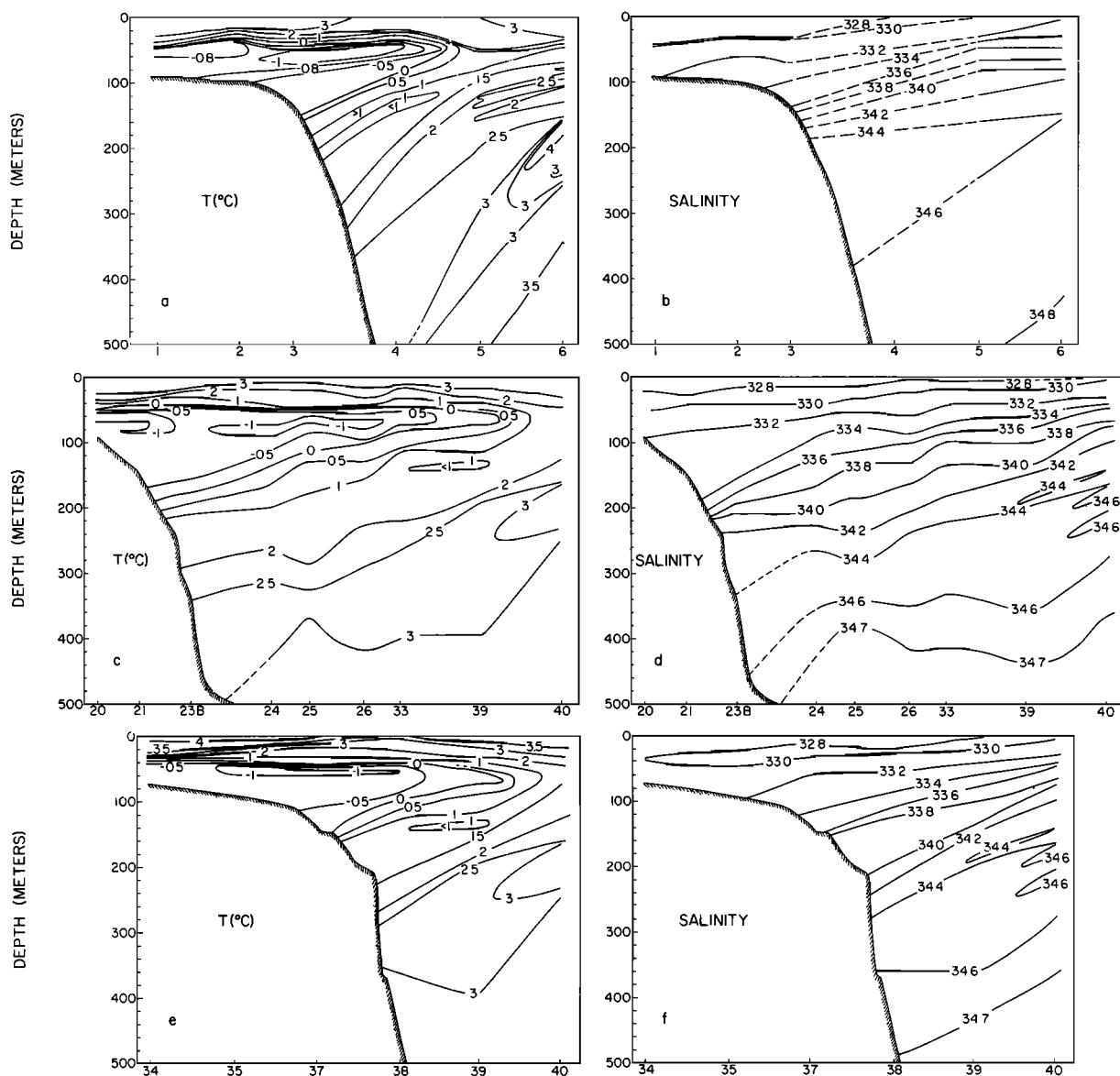


Fig. 2. The 1980 temperature and salinity sections: (a and b), northeastern; (c and d), central axis; and (e and f), southwestern. The broken lines signify lack of data.

meters (Figures 6b and 6c) exhibit tidal modulation similar to that in Figure 3a. This tidal modulation is nearly absent in the record from the downstream meter (Figure 6a).

All instruments registered a marked increase in temperature shortly after midday on June 9. At the downstream meter, for which the effect was most pronounced, the mean temperature increased from near -1°C to almost 2°C in less than a day and then gradually returned to the previous values over the next 5 days. A similar response (i.e., an abrupt temperature increase followed by persistently higher temperatures for a 6-day period) is present in the records from each of the central axis and upstream instruments (Figures 6b and 6c). Because increased salinities were also registered by each instrument during the event [Kinsella, 1984], the observed warm water could not have had a shallow-water origin.

The maximum change in average temperature at the central axis meter is significantly less than that at either of the meters near the shelf break. It is also noteworthy that prior to the

event the highest mean temperatures were registered by the central axis instrument (Figure 6b), the mean temperatures at the other two instruments being about 0.7°C lower. This pattern is consistent with the temperature field in 1980 (Figure 2) at the depths of these instruments. During the event, however, the pattern is different: on June 10, for instance, the highest mean temperatures registered near the shelf break by the downstream and upstream meters were higher or about the same, respectively, as that at the central axis mooring.

Vertical ascent rates of isohalines during the initial period of rapid temperature and salinity change were computed at the central axis mooring from the current meter record and a CTD profile taken prior to the event on June 6 at the central axis mooring location. The ascent rate for the 33.99 isohaline was 0.7 cm s^{-1} : from 229 m to 168 m in 2.5 hours [Kinsella, 1984]. This rate of ascent is comparable to or larger than the maximum vertical velocities measured by Shaffer [1976] using neutrally buoyant floats within an upwelling zone centered

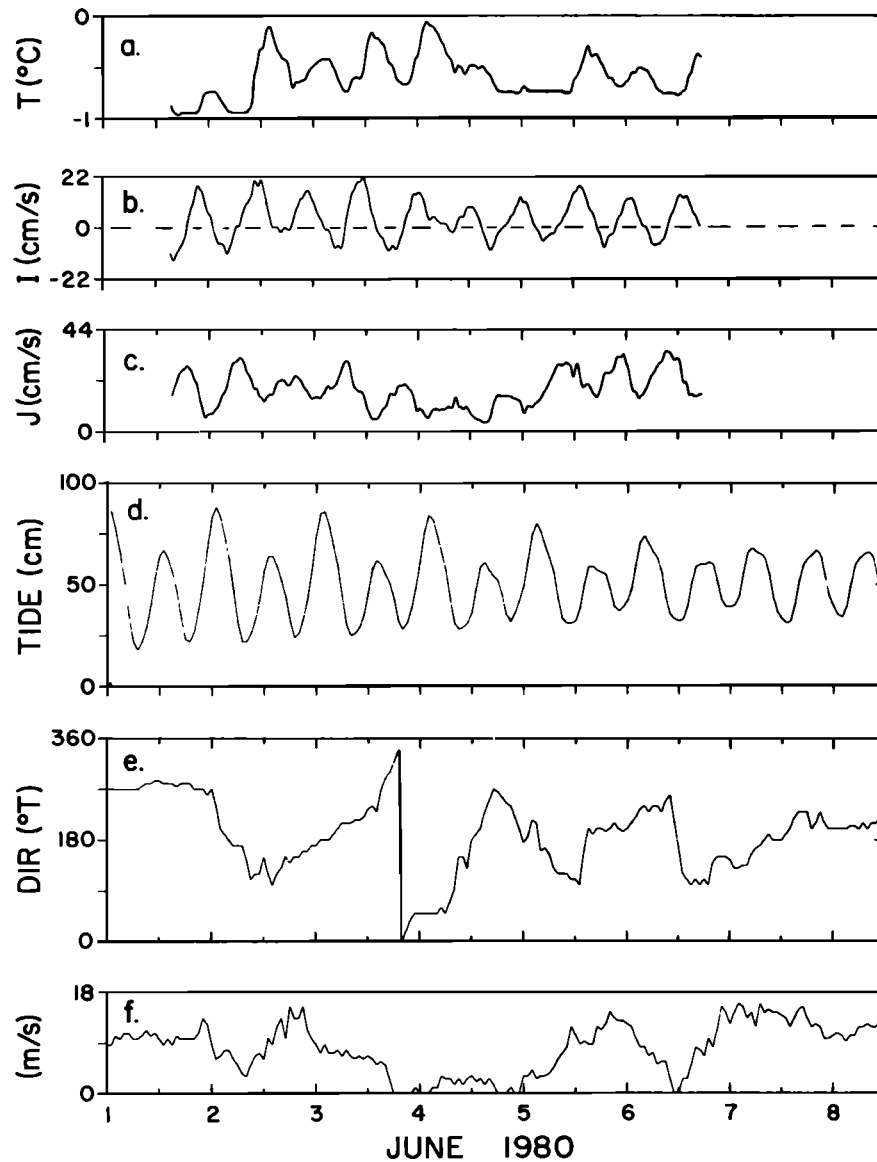


Fig. 3. The 1980 current meter records, tides, and winds: (a) temperature, (b) cross-isobath velocity, positive along $280^\circ T$, and (c) along-isobath velocity, positive along $190^\circ T$, velocity from the southwestern meter; (d) tidal elevation; and (e) the wind direction (from); and (f) wind speed at 84-m height at Hibernia. The time series begin at 0000 UT on June 1, 1980.

over the head of a submarine canyon off the northwest coast of Africa. It is also comparable to the maximum vertical velocity (0.2 cm s^{-1}) estimated by *Petrie* [1983] from the storm-driven ascent rates of isotherms near the shelf break off Nova Scotia.

The winds measured at Hibernia during the period of the experiment are presented in Figures 7a and 7b. A storm passed through the region on June 8 and 9. Winds changed to southeasterly (on shelf), increased rapidly to gale force values of up to 24 m s^{-1} early on June 8, and then shifted abruptly to southwesterly (along shelf and upwelling favorable) near midday on June 8. These abrupt changes at high speeds are to be compared with the wind data from the previous year in Figures 3e and 3f, when no upwelling was observed, and which were described as low speed and slowly varying in section 3.1. The southwesterly winds persisted at sustained, but

lower ($12\text{--}16 \text{ m s}^{-1}$), speeds until early on June 10. Wind speeds of this magnitude, blowing from the southwest to northwest directions, continued at intervals until midday on June 13, at which time speeds dropped below 10 m s^{-1} and remained below this level for the duration of the experiment. The sea level atmospheric pressure fields during the storm immediately prior and subsequent to the shift to southwesterly winds are presented in Figures 7c and 7d. It can be seen that the storm was associated with a low-pressure center moving northeastward across the island of Newfoundland and that the shift from intense southeasterlies to weaker southwesterlies observed at Hibernia is consistent with the changes in the pressure field. Furthermore, the curvature of the isobars suggests that at points south and west of Hibernia, such as Carson Canyon and its vicinity, the strongest winds may have had a relatively stronger southerly component. Otherwise, it

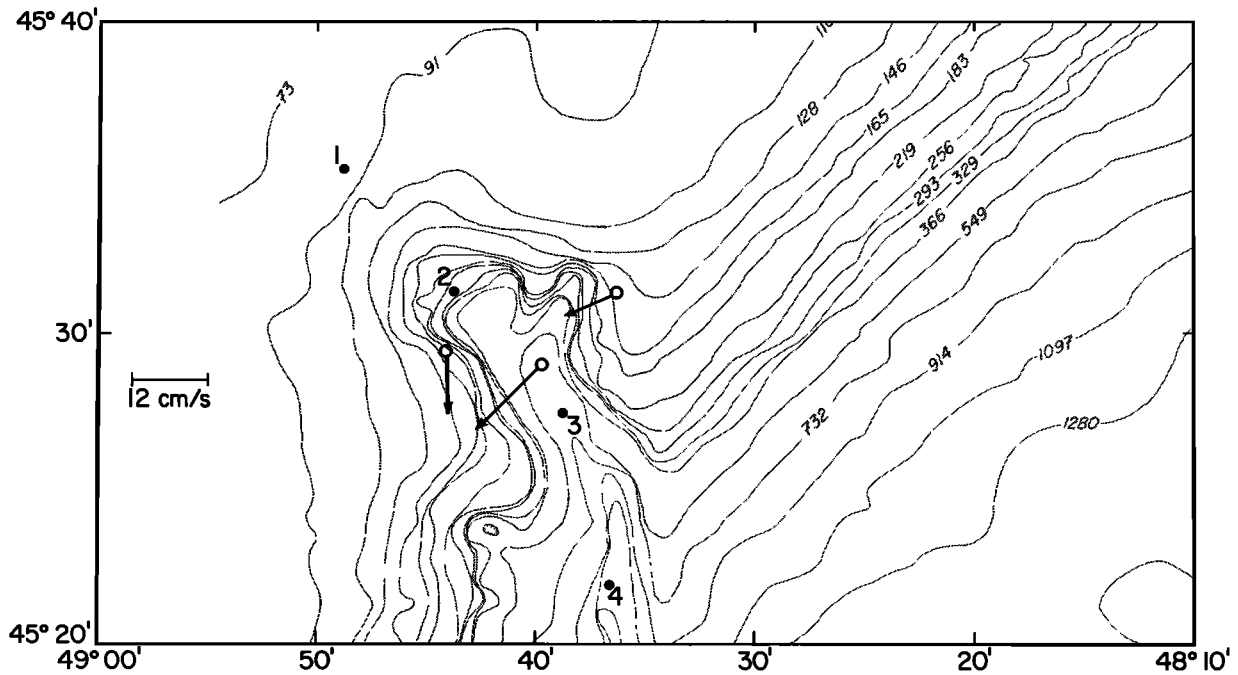


Fig. 4. The 1981 CTD stations and current meter mooring locations, with mean current vectors during June 4–7 at shelf break depth.

would appear that much the same wind field as that observed at Hibernia should have occurred at Carson Canyon.

We now consider the response of the velocity field at shelf break depth. Since there exist very few measurements with a coherent current meter array of time-varying flow in the vicinity of a canyon, we make a detailed presentation of our data. The changing velocity field is presented as 12-hour segment-averaged vectors (Figure 8) and in the form of progressive vector diagrams (Figure 9). Both Figures 8 and 9 were con-

structed from the 33.2-hour low-pass-filtered velocity components for each instrument. The segment-averaged vectors illustrate the changes in the velocity field relative to the bathymetry as a function of time at all three sites. The progressive vector diagrams convey more readily the continuous changes in direction which occurred at each site. The following discussion refers to both Figures 8 and 9.

At all three current meter locations the measured currents exhibit pronounced changes in speed and direction at some

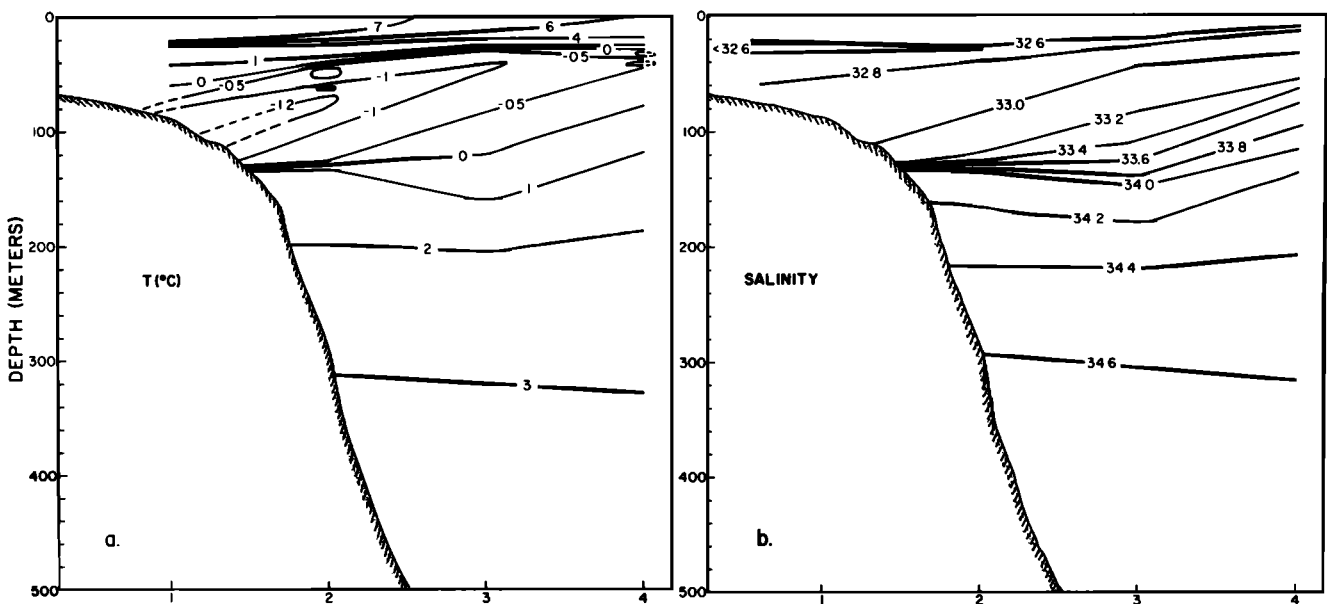


Fig. 5. (a) Temperature and (b) salinity sections along the central axis on June 11, 1981.

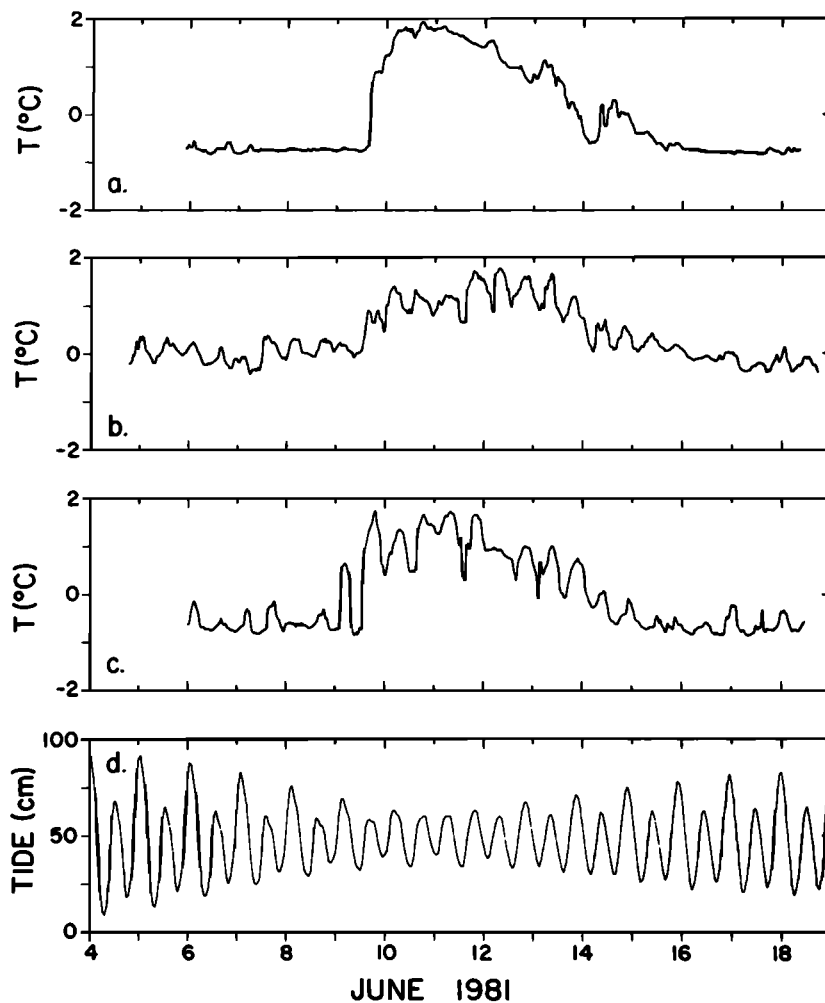


Fig. 6. Temperature time-series from the current meters at shelf break depth in 1981: (a) downstream, (b) central axis upper, and (c) upstream; along with (d) the tidal elevations at Hibernia. The time series start at 0000 UT on June 4, 1981.

point during June 8–15, which spans the period of upwelling, but return subsequently to preevent values. The timing and magnitude of the changes were different at each location, however. Examining Figure 9, for example, flow reversal or near-reversal occurred at all three instruments, first at the downstream and upstream meters early on June 8, and subsequently at the central axis meter on June 9. The period of reversed and variable flow roughly corresponds to, but tends to occur earlier than, the period of elevated temperatures in Figure 6. A glance at either Figure 8 or 9 shows that there are large spatial differences in velocity over rather small distances during the event.

More precise determination of the time of the event's onset is necessary before proceeding. This is best defined in terms of changes in the velocity field, which must result initially from the barotropic response and therefore occur earlier than changes in density. Figures 8 and 9 suggest that the onset is characterized by deceleration and subsequent reversal or near-reversal of the mean flow from its dominantly along-isobath direction at the downstream and central axis moorings and the cross-isobath direction at the upstream mooring. These components (1.4-hour cutoff low-pass filtered) are plotted in Figure 10. The effect of the event is most prominent in the

record from the central axis instrument. At each mooring, reversal of the mean occurs during the early part of the event, although at the central axis meter (Figure 10b) the reversal occurs later and is more prolonged than at the other two instruments. A period of deceleration prior to reversal is evident in each record. At the downstream and upstream instruments (Figures 10a and 10c, respectively; see also Figure 8), this deceleration begins during the first half of June 8; that is, during the period of high-speed winds (Figure 7). These velocity changes occur at least a day before the abrupt temperature change at the downstream meter (Figure 6). At the central axis mooring, deceleration occurs later (during the latter half of June 8). At the central axis the association between elevated temperatures and reversed or near-zero cross-canyon flow is quite clear.

The times at which the velocity changes occurred suggest that the time of onset was between about 0600 and 1200 UT on June 8. The delay between the time of reversal and the onset of pronounced temperature and salinity increases at the shelf break is, in the case of the downstream instrument, very likely the result of the temperature and salinity fields being locally homogeneous, since no tidal modulation of the time series of these scalar quantities was observed at this location

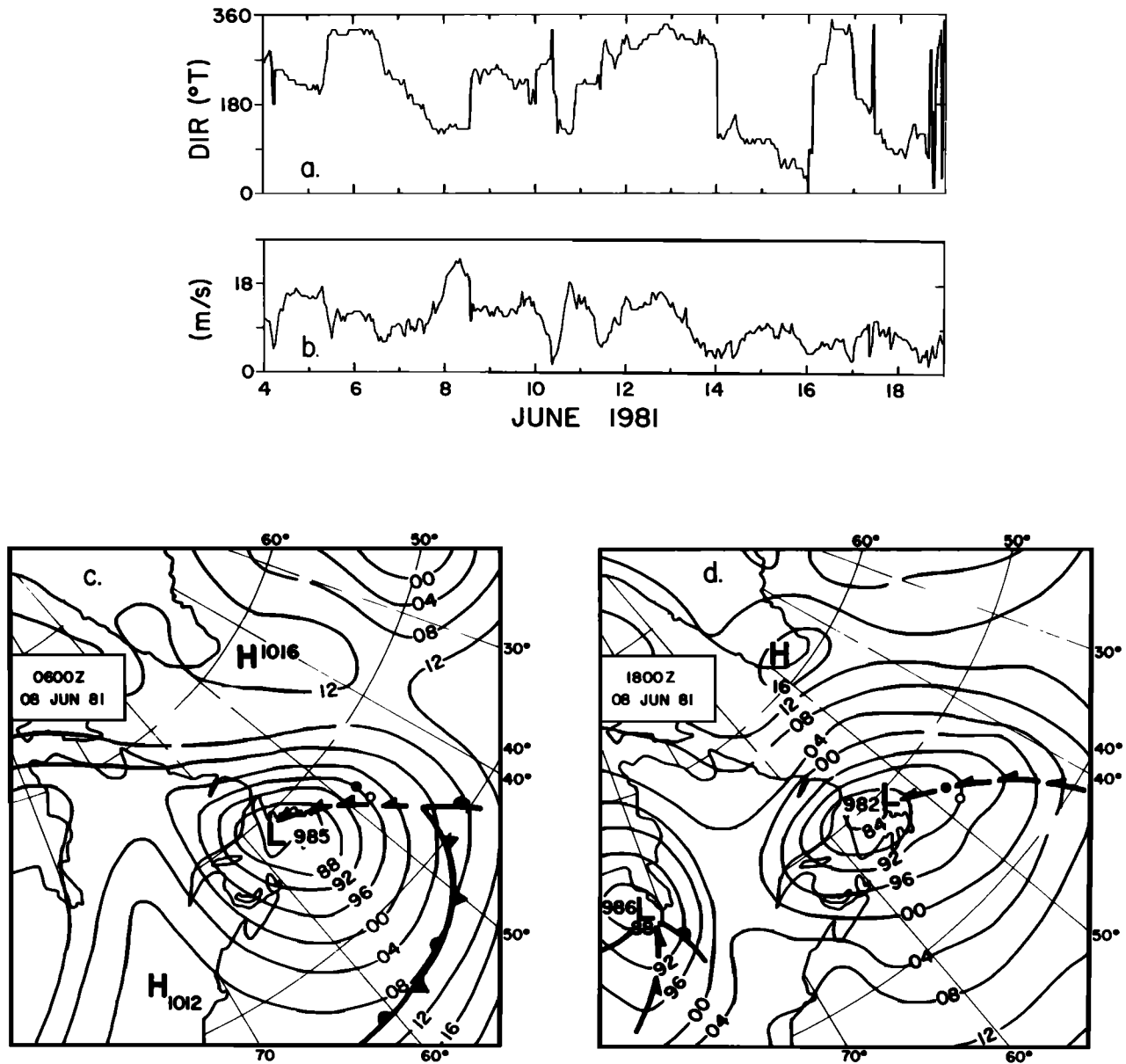


Fig. 7. (a) Wind direction (from) and (b) wind speed at 84-m height at Hibernia in 1981, along with surface pressure charts for June 8 (c) at 0600 UT and (d) at 1800 UT.

(Figure 6a). In contrast, at the upstream instrument the time at which the temperature increase first begins is masked by tidal variations (Figure 6c).

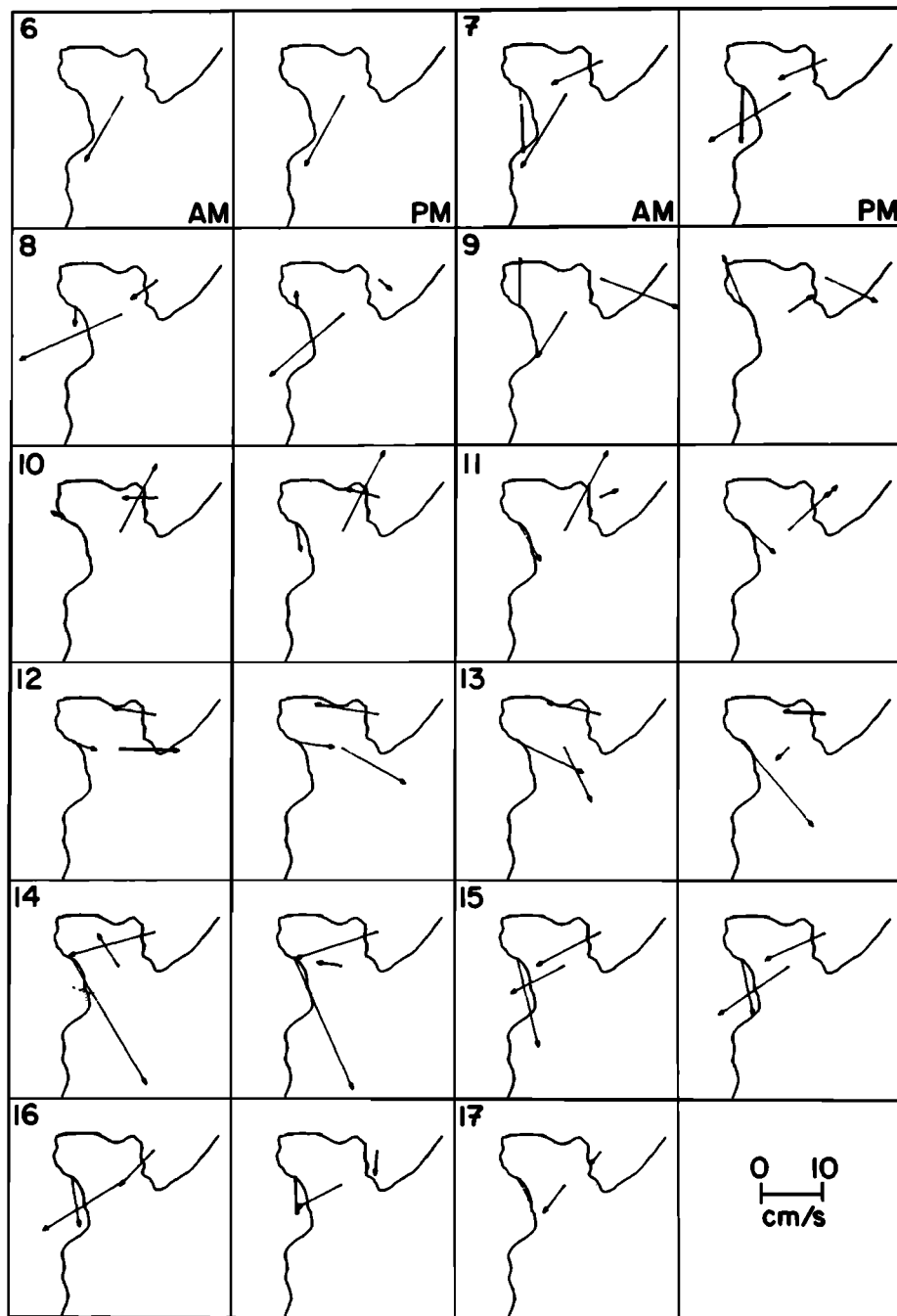
4. DISCUSSION

4.1. Upwelling Event

We investigate the possibility that the event was due to upwelling during the storm and begin by examining the time and space scales. The characteristic offshore length scale of the baroclinic response in wind-driven upwelling problems is the internal deformation radius a' . Approximating the density stratification by a two-layer system in which the thickness h of the upper layer is very much less than that of the lower layer, $a' = (g'h)^{1/2}/f$, where g' is the reduced acceleration due to gravity, f is the Coriolis parameter, and $(g'h)^{1/2} = c'$ is the phase

speed of long interfacial waves. From Figure 5, $h \approx 100$ m and $g' \approx 5 \times 10^{-3} \text{ m s}^{-2}$, giving $c' = 0.7 \text{ m s}^{-1}$ and, with $f = 10^{-4} \text{ s}^{-1}$, $a' = 7 \text{ km}$. This is reasonably close to the width of the zone of uplifted isopleths in Figure 5, supporting the upwelling hypothesis. Further support is provided by the smaller temperature change registered at the central axis mooring compared to that at the shelf break instruments: this diminished but significant response is expected at this mooring, since it was located about 5 km (less than a') from the shelf break.

In the case of upwelling along an infinite coastline driven by an impulsively started uniform wind stress, the e -folding time of the initial adjustment to steady on-offshore motion is $O(1/f)$, which is the time required for an interfacial wave to travel a distance equal to a' (see, for example, Gill [1982], pp. 386, 404). This time scale is about 3 hours at the latitude of Carson Canyon.



12 HR. START 23:30Z 5/06/81. 1CM=10CM/SEC

Fig. 8. The 12-hour segment-averaged velocity vectors from the instruments at shelf break in 1981.

In the presence of a topographic irregularity with length scale L , say, there will exist a second time scale governing the response in the vicinity of the irregularity given by the time required for an interfacial wave to travel the distance L . Because the width of Carson Canyon is comparable to the internal deformation radius, the baroclinic response near the shelf break will be governed in part by internal Kelvin waves propagating around the canyon edge. This is a distance of about 30 km along the isobaths between 100 and 200 m. The associated topographic time scale should therefore be about 12 hours.

The total range of locally controlled time scales is therefore

3–12 hours. As discussed previously, the time of onset of the event was between 0600 and 1200 UT on June 8 at the shelf break instruments and later on June 8 at the central axis mooring location. These time scale estimates are therefore consistent with the interpretation that the event was due to the abrupt increase in wind speeds near 0000 UT on June 8 (Figure 7). The delayed response at the central axis can be interpreted as being due to the additional time required for a significant response to develop away from the shelf break at the depth of this instrument.

These considerations lead us to suggest that the event was

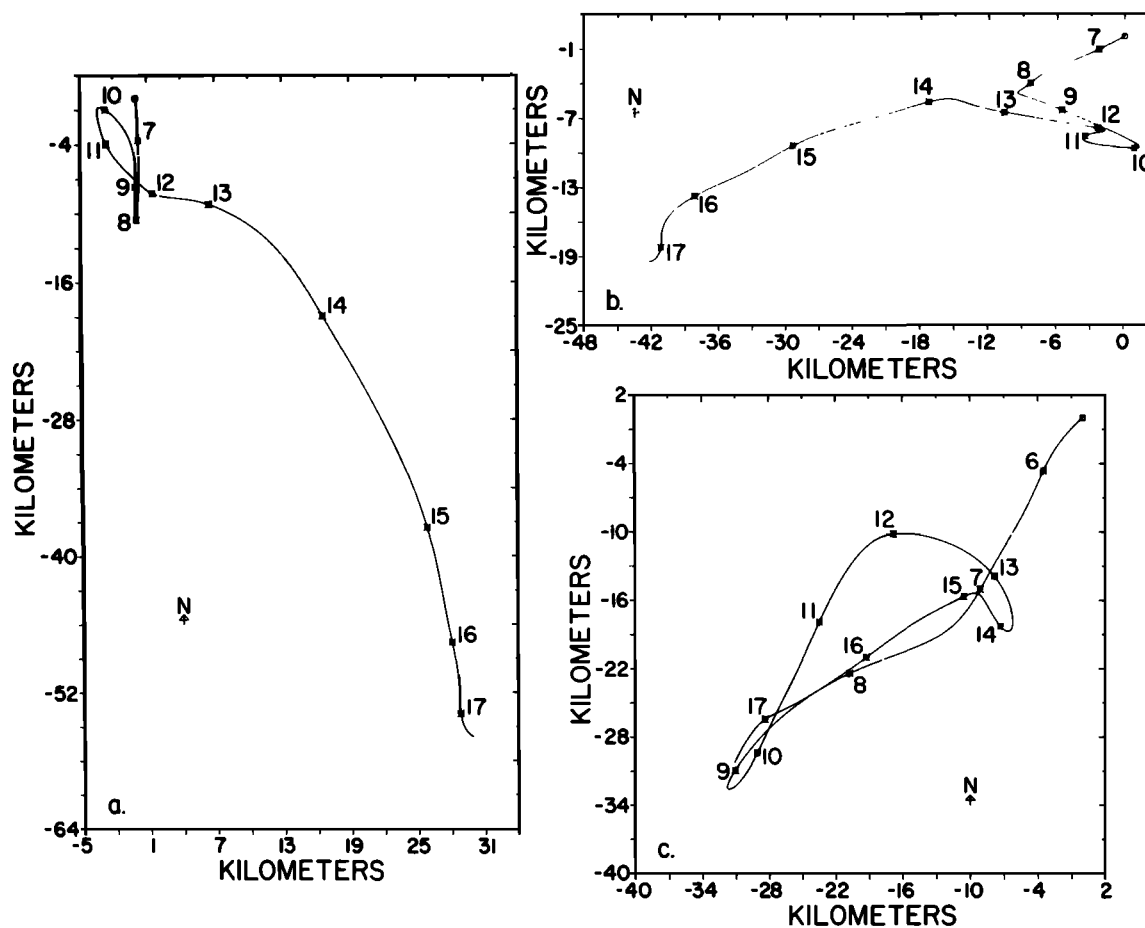


Fig. 9. The 1981 progressive vector diagrams for (a) the downstream, (b) the upstream, and (c) the central axis upper current meters.

probably due to wind-induced upwelling at the head of the Canyon. One of the uncertainties in this interpretation is the absence of direct measurements of the vertical structure of the currents. Vertical profiles of geostrophic velocity were therefore constructed and are presented in Figure 11 relative to the 200-dbar surface. The profiles shown are that during the event (solid line) on June 11, 1981, for stations 2 and 3 (Figure 4) and that in June 1980 (dashed line) for stations 23 and 24 (Figure 1b). Positive speeds are directed toward the southwest. The principal difference between the two profiles is the presence of northeastward flow in the 1981 profile between 100- and 180-m depth, which is consistent with the reversed flow registered by the central axis meter at this time (Figures 8–10). Above this depth range the Labrador Current continued to flow toward the southwest. These data indicate therefore that the reversals observed at the upstream and downstream moorings near the shelf break were probably confined to the near-bottom zone and that the southwestward flow of the Labrador Current continued in the overlying shallow water, probably at reduced speeds.

The flow reversals themselves were probably associated with the barotropic response to the applied wind stress. They were initiated prior to the onset of increased temperatures and persisted for comparable, although somewhat shorter, time scales. The reversals were directed roughly parallel to the shelf break in the poleward direction. This is the direction of the

barotropic response to an upwelling favorable wind at a western boundary.

4.2. Mean Flow

In this section we examine the mean flow-canyon interaction problem. The discussion is restricted primarily to characterizing the important terms in the momentum and vorticity balances.

The dynamic topography in 1980 of the 5-dbar surface relative to 200 dbar is presented in Figure 12. Only the data from stations deeper than 200 m are presented. By examining the 85 and 90 dyn. cm (dynamic centimeter) contours, it is seen that for water depths greater than 500–600 m, these data indicate that the canyon exerts little influence on the Labrador Current, whereas in shallower water the dynamic topography exhibits pronounced shelfward deflections over Carson Canyon and the smaller canyon downstream. In deeper water over the slope the Labrador Current is apparently shielded from the effects of topographic variations by the stratification. Shelfward of the 500-m isobath, however, the current feels the bottom, and topographic effects are large.

There are two caveats with respect to Figure 12. Dynamic heights computed from a 25-hour time series of CTD's at station 1 (Figure 1b) show peak-to-peak variations of 2 dyn. cm at the frequency of the semidiurnal tide [Kinsella, 1984]. The dynamic topography in Figure 12 may be aliased as a

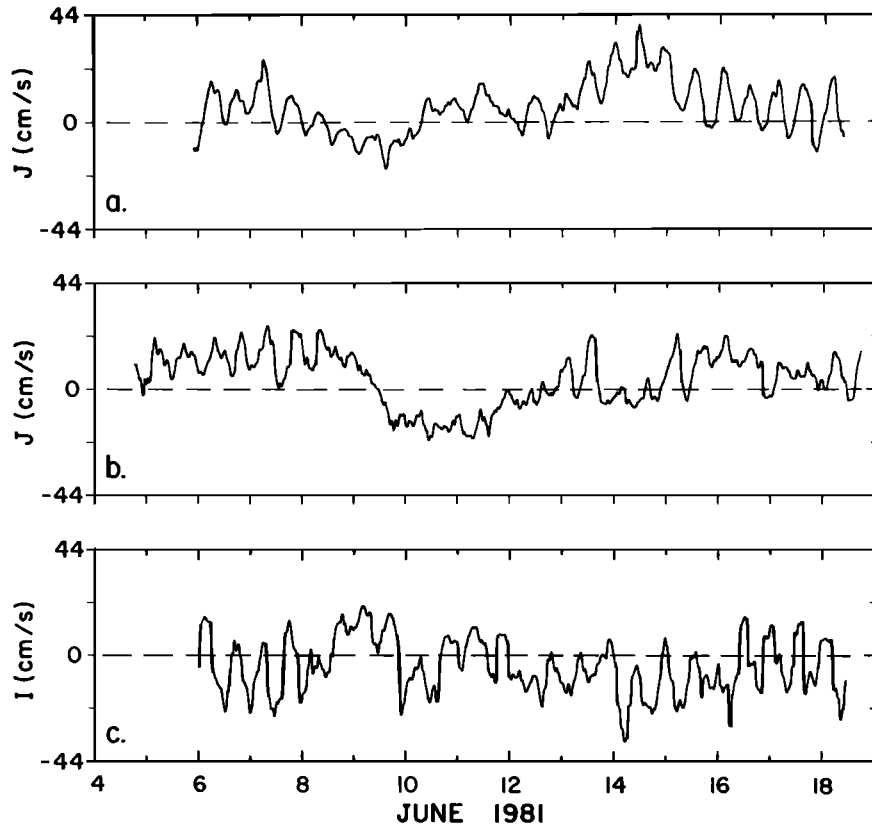


Fig. 10. Time series in 1981 of (a) the along-isobath velocity component from the downstream current meter (positive along $150^\circ T$); (b) the along-isobath component from central axis upper current meter (positive along $210^\circ T$); and (c) the cross-isobath component from the upstream meter (positive along $80^\circ T$).

result. However, since the CTD data were collected over a 5-day period at irregular intervals, the effects of tidal aliasing are not thought to be severe. The second caveat is that ageostrophic effects associated with the canyon topography appear to be important, as discussed later, so that interpretation of the dynamic height contours in Figure 12 as streamlines is not strictly valid. It should be mentioned that these same caveats also apply to Figure 11.

Now consider the 1981 current measurements in Figures 8 and 9. On June 6 and 7, prior to the upwelling event, the mean flow is cross canyon at the central axis mooring, is cross isobath and into the canyon at the upstream mooring, and is directed along and shelfward of the canyon wall on the down-

stream side. The same pattern recurs on June 15–17, after the event, indicating that although the magnitudes of the velocities change, these directions may be representative of mean flow conditions. The mean currents during the period prior to the event are shown in Figure 4.

The magnitudes of the nonlinear terms in the momentum balance were estimated from the segment-averaged velocity vectors on June 7 prior to the upwelling event (Figure 8). Using the measured mean velocity components at the central axis location for the advective speeds and Coriolis accel-

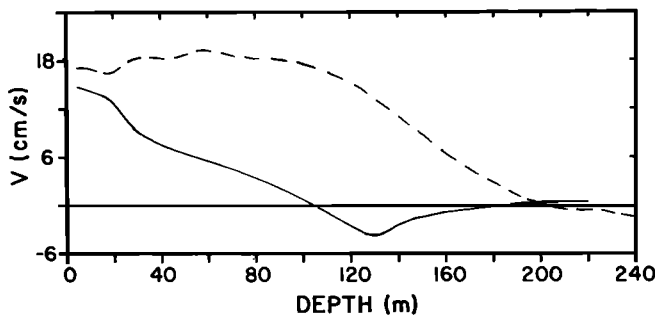


Fig. 11. Vertical profile of geostrophic velocity between CTD stations 2B and 3 in 1981 (solid line), and between 23B and 24 in 1980 (dashed line).

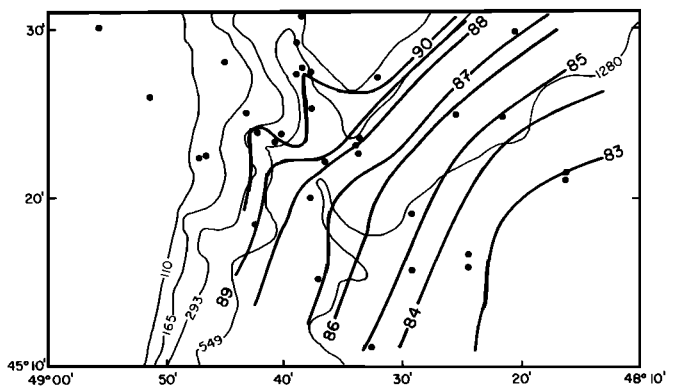


Fig. 12. Dynamic topography (heavy lines) of the 5-dbar surface relative to 200 dbar in dynamic centimeters. Numerical values equal dynamic height less 18,900. The solid circles are the 1980 CTD station locations.

ations, and the differences between these speeds and the components measured at the other two locations to calculate gradients, we obtained estimates for the four Rossby numbers: $Ro^{xx} = uu_x/fv$, $Ro^{xy} = vu_y/fv$, $Ro^{yx} = uv_x/fu$ and $Ro^{yy} = vv_y/fu$. In these expressions, u is the velocity component in the x direction, which is taken to be positive onshelf ($315^\circ T$), v the component in the along-shelf direction y , which is positive southwestward ($225^\circ T$) and parallel to the line joining the upstream and central axis mooring locations. The subscripts denote partial differentiation. All values were found to be small (<0.2) except Ro^{yy} which, depending on the pair of moorings or the half-day chosen, ranged from 0.4 to 0.7. This indicates that the nonlinear term vv_y should be retained in the cross-canyon momentum balance.

Note that we have implicitly assumed in the previous discussion that the current measured at 10 m above bottom is representative of the interior flow: that is, it is not greatly affected by friction. This question is pursued in the appendix, where it is shown that in these circumstances the measured mean current is probably within 10% of the interior value. This is close enough for our purposes.

In order to investigate the vorticity balance we adopt a two-layer representation of the Labrador Current, with the lower layer at rest. The interface is taken to coincide roughly with the 34.0 isohaline, which is below the low-temperature core of the Labrador Current (Figure 2). This isohaline intersects the bottom at about 200-m depth (Figure 2f) and hence in this representation the flow is barotropic shelfward of the 200-m isobath. The steady, nonlinear inviscid shallow-water (hydrostatic pressure, u and v depth independent) equations are used to describe flow in the interior far from the bottom boundary. The bottom boundary layer thickness is denoted by δ . Following the usual procedure [e.g., Gill, 1982, p. 231] we obtain the equation governing the potential vorticity of the interior flow:

$$\mathbf{u} \cdot \nabla \left[\frac{\zeta + f}{H^* + \eta} \right] = - \frac{(\zeta + f)}{(H^* + \eta)^2} q_E \quad (1)$$

where q_E is the velocity normal to the interface between the interior and the boundary layer at $z = -H^* (= -H + \delta)$, η is the free surface elevation, $\zeta = v_x - u_y$ is the relative vorticity, and

$$\mathbf{u} \cdot \nabla = u \frac{\partial}{\partial x} + v \frac{\partial}{\partial y}$$

In the bottom boundary layer the equations of motion are written in a rotated frame of reference (x' , y' , z') such that z' is normal to the bottom, and y' is in the along-isobath direction. The equations of motion become

$$-\hat{f}v' = -\frac{1}{\rho} p'_{x'} - g \sin \alpha + \frac{1}{\rho} \frac{\partial \tau^{x'}}{\partial z'} \quad (2a)$$

$$\hat{f}u' = -\frac{1}{\rho} p'_{y'} + \frac{1}{\rho} \frac{\partial \tau^{y'}}{\partial z'} \quad (2b)$$

where α is the bottom slope, $\hat{f} = f \cos \alpha$, and α is assumed to be sufficiently small that the additional Coriolis accelerations involving $f \sin \alpha$ in the y' and z' directions can be ignored. Cross differentiating (2) and vertically integrating after making use of the continuity equation gives, for constant α ,

$$q_E = \frac{1}{\rho \hat{f}} (\tau_{ox'}^{y'} - \tau_{oy'}^{x'}) \quad (3)$$

which is the Ekman pumping velocity due to the curl of the bottom stress ($\tau_{ox'}^{y'}$, $\tau_{oy'}^{x'}$). Strictly speaking, (3) is valid only for small Rossby numbers, since (2a) and (2b) are linear. This is not a difficulty for the applications considered here, however, since it will be shown that bottom torque appears to be important only when the nonlinear terms are small. For small α , (3) is approximated by $(\tau_{ox'}^{y'} - \tau_{oy'}^{x'})/\rho f$ and, when combined with (1), becomes

$$-H(u\zeta_x + v\zeta_y) + (\zeta + f)(uH_x + vH_y) = (\zeta + f)(\tau_{ox'}^{y'} - \tau_{oy'}^{x'})/\rho f \quad (4)$$

where it has been assumed that $\eta \ll H$, $\delta \ll H$, and gradients of δ are small in comparison with gradients of H . Pedlosky [1979, p. 223] has derived a similar vorticity equation for the small Rossby number case in which u and v assume their geostrophic values. We now examine the implications of this balance both upstream of and at the canyon.

4.2.1. *The far field.* Holton [1979, p. 91] has discussed the problem of uniform westward flow over a ridge of finite width and infinite north-south extent on a β plane in the northern hemisphere. He shows that fluid columns must begin to veer to the left upstream of the ridge. Using the same argument for an infinite trench, it would be expected that a fluid column would veer to the right before reaching the trench. In the present situation, β is not important, but since the geometry involves flow toward the canyon with shallow water on the right, the cross-stream depth gradient can be expected to play an analogous role. Pedlosky [1979, pp. 94–99] discusses flow toward a wall in this context and finds that rightward veering begins in an inertial boundary layer on the upstream side, with a thickness λ given by

$$\lambda = \left(\frac{vH}{-fH_x} \right)^{1/2} \quad (5)$$

Substituting $H = 100$ m, $v = 20$ cm s $^{-1}$, and $H_x = 10^{-2}$ (Figure 1b) in (5) gives $\lambda \sim 5$ km.

There is another scale which could control the distance upstream at which veering begins, and that is the width of the canyon. Hogg [1980] has discussed the problem of flow over a circular bump on a flat bottom on an f plane. Veering to the left, or to the right for a circular depression, begins upstream at a distance which depends on the magnitude of the ratio of bump height scaled by water depth to the Rossby number based on the bump radius. In the two-layer representation used here, Carson Canyon and the motionless lower layer effectively form a depression about 100 m deep, with a diameter roughly equal to the canyon width. The scale depth of the depression is therefore about 1. The Rossby number based on canyon half width is about 0.4. The ratio of these is therefore roughly 2, and significant rightward veering would be expected to occur at about one or two radii upstream, or 5 to 10 km.

Both scales are therefore the same magnitude. Because of the cross-stream depth gradient in the present problem, however, we believe that the inertial boundary layer thickness is the more appropriate choice. Its existence is related to the facts that at the canyon the constraint that the flow follow contours of f/H must be broken even in the absence of friction and that topographic Rossby waves cannot propagate upstream [see Pedlosky, 1979, p. 109]. The far field is defined as the region outside this boundary layer.

Examining Figure 1b, it is seen that the distance from the upstream mooring to the point at which the isobaths begin to curve sharply shelfward at the Canyon is also about 5 km. The shelfward veering of the mean flow observed at this location may therefore be due at least in part to the presence of Carson Canyon. A different explanation, however, must exist for the shelfward flow observed at the downstream mooring, since both the infinite trench and circular depression arguments would result in veering into deeper water on the downstream side.

In the far field, $\zeta \ll f$, and along-shelf gradients should be much weaker than cross-shelf gradients. Accordingly, the $\partial/\partial y$ terms in (4) are dropped, yielding

$$-Huv_{xx} + fuH_x = \tau_{ox}^y/\rho \quad (6)$$

The ratio of the advective and stretching terms is Hv_{xx}/fH_x . Using 20 km for the cross-stream length scale, which is the half width of the Labrador Current [Petrie and Anderson, 1983], and the same values as given earlier for the other parameters, this ratio is about 0.05. Advection of relative vorticity can therefore be ignored in the far field and (6) becomes

$$uH_x = \tau_{ox}^y/\rho f \quad (7)$$

This result has potentially important implications for on-off-shelf exchange in the region. The Labrador Current velocity maximum is located seaward of the shelf break and is often associated roughly with the 500-m isobath [e.g., Mountain, 1980]. The doming of the 3° isotherm to meet the surface over the 500-m isobath in Figures 2a and 2e may reflect this. Regardless, the point is that v_x is expected to be negative at the shelf break. Writing the bottom stress as $\tau_o^y/\rho = C_d v^2$, it is clear from (7) that since H_x is also negative, $u > 0$, and there should be a mean flow onto the shelf at the shelf break. Using 20 km as a typical cross-stream length scale as before, $H_x = -2 \times 10^{-2}$ at the location of the upstream mooring (Figure 1b), and $v = 20 \text{ cm s}^{-1}$; (7) gives $u = 0.6 \text{ cm s}^{-1}$ with $C_d = 3 \times 10^{-3}$. This gives a shelfward deflection angle $\tan^{-1}(u/v)$ of about 2°. Larger values are obtained by using v_o , the velocity at the jet axis, as the velocity scale for the cross-stream shear: this gives $u = 1.5 \text{ cm s}^{-1}$ and a deflection angle of 4.3°. The 13°–14° on-shelf veering observed at the upstream and downstream moorings (Figure 1b) is therefore probably only partly due to this effect.

The implied on-shelf transport is significant: at least $60 \text{ m}^3 \text{ s}^{-1}$ per 100 m along-shelf distance. For comparison, this is similar to typical monthly averaged wind-driven on-off-shelf Ekman transports [e.g., Bakun, 1975]. Furthermore, Petrie and Isenor [1985] have estimated the on-shelf volume transport in the Grand Banks region from the trajectories of satellite-tracked drifters. They obtained a value of $40 \text{ m}^3 \text{ s}^{-1}$ per 100 m of shelf, which is comparable to that given previously, and found by the use of a box model that it should significantly influence the mass balance on the shelf and the on-shelf flux of icebergs. They suggested that the transport is caused by eddies generated through baroclinic instability. The eddy flux is undoubtedly important. For example, since the above transport (equation (7)) is driven where v_x is nonzero and therefore could vanish at the nearshore limit of the Labrador Current, the eddy flux would then be necessary for the icebergs to diffuse away from the edge of the current onto the shelf. Nevertheless, the calculation above indicates that the flux of icebergs and other scalar quantities across the Lab-

rador Current induced by Ekman suction in the bottom boundary layer may be important.

4.2.2. *The near field.* The previous discussion with respect to the Rossby numbers suggests that the important advective term in the near field is $v\zeta_y$ (advection of relative vorticity into the canyon). The ratio of advection to stress curl in (4) therefore becomes

$$\frac{H\zeta_y}{2C_d\zeta} = \frac{H}{2C_dL} \quad (8)$$

where L is a cross-canyon length scale governing the change in relative vorticity. Setting $L = 5 \text{ km}$, half the canyon width, and with $C_d = 3 \times 10^{-3}$ and $H = O(100 \text{ m})$ gives a value of slightly more than 3 for this ratio. The value of H is a lower bound, however, suggesting that the ratio could in fact be twice as large.

We therefore assume that friction can be ignored in the vorticity balance in the near field. Equation (1), with q_E set to zero, η small, and $H^* \approx H$, reduces to the usual result that $(\zeta + f)/H$ is constant along streamlines. Letting U be the speed along a given streamline and R its radius of curvature, the relative vorticity is given by

$$\zeta = -\frac{\partial U}{\partial R} - \frac{U}{R} \quad (9)$$

Consider the 165-m isobath in Figure 1b. Immediately upstream of the canyon, its radius of curvature is about 2 km. Assuming that $-\partial U/\partial R$ retains the same sign as the vorticity upstream (i.e., negative) and that $U \sim 20 \text{ cm s}^{-1}$, (9) indicates that if the flow were to follow the isobaths, $-U/R$ and therefore ζ would become comparable but opposite in sign to f . The flow must therefore move into deeper water to produce a compensating positive relative vorticity through vortex stretching.

We now turn to the argument presented by Holton [1979, p. 91] for uniform flow over an infinite ridge and apply it to uniform flow over a canyon of finite length and width with shallow water to the right. The depth gradients parallel to the canyon axis in both the near and far fields play the role of β . The flow must acquire negative relative vorticity upstream, and it does so by veering to the right in the inertial boundary layer. (Were this not to happen, so that the flow encountered the canyon with no relative vorticity, it would instead have to veer to the left as depth increased over the canyon, which would bring it into deeper water still, requiring increased leftward curvature, until the flow direction was reversed.) The negative vorticity acquired by the flow in the inertial boundary layer is balanced by the associated decrease in depth as fluid columns veer to the right. On the upstream side of the canyon, fluid columns encounter an increase in H requiring that ζ increase: that is, rightward curvature is gradually removed, and the flow eventually veers to the left to cross the canyon. Over the canyon axis the flow is parallel to the isobaths, and on the downstream side the process is repeated but in the opposite sense. The resultant streamlines are symmetric about a canyon symmetric about its axis, and on the upstream side, cross isobaths into shallower water in the inertial boundary layer and into deeper water over the canyon wall. The mean flow pattern indicated by the measured mean currents in Figure 4 is consistent with this: cross-isobath flow into deeper (shallower) water on the upstream (downstream) side and cross-canyon flow over the axis. The lack of symmetry in the

measurements could be due to the asymmetric canyon shape, resulting especially from the secondary canyon on the upstream side, the nonzero relative vorticity in the far field upstream, and/or stratification.

This model suggests that scalar quantities found at a given depth upstream should, in the absence of diffusion, be located in deeper water over the canyon axis and return to shallow water on the downstream side. Examining the temperature and salinity sections for Carson Canyon in Figure 2, it is seen that this is in fact the case. The 0° isotherm, for example, intersects the bottom at roughly 150 m on the upstream side, 190 m over the axis, and somewhat less than 150 m on the downstream side. An estimate of the maximum depth change to be expected can be made on the basis of the above model by setting the relative vorticity at the axis equal to its maximum possible value U/R , R being the radius of curvature of the isobaths at the canyon head, and equating the potential vorticity at the axis with that in the far field upstream. From Figure 1b, $R \sim 4$ km for isobaths in the vicinity of 200 m, giving $\zeta \sim 0.5f$ at the axis. With H being the depth upstream, this gives $1.5H$ as the depth to which fluid columns would move at the axis. For the case considered here ($H = 150$ m), the maximum depth change expected at the axis would therefore be 75 m. Given the uncertainties and the fact that the effects of far field relative vorticity, bottom friction, and stratification have been ignored, this is in satisfactory agreement with the 40 m observed.

Over the central part of the canyon the total water depth increases (713 m at the central axis mooring), and the effects of stratification are expected to become more important. In fact, it appears that the upstream flow may be supercritical. The internal Froude number is given by

$$F_i = \frac{V}{N_0 H} \quad (10)$$

where N_0 is the buoyancy frequency. Here we have employed the expression for F_i used by Long [1953], who found that flow of a continuously stratified (nonrotating) fluid of finite depth over a ridge was supercritical for $F_i > \frac{1}{3}$. Using $N_0^2 \approx 6 \times 10^{-8} \text{ s}^{-2}$ (Figure 2f), $H = 150$ m for a typical upstream water depth, and $V = 20 \text{ cm s}^{-1}$ for the upstream mean speed, (10) gives a value of 5 for F_i . This is certainly supercritical using Long's criterion. Although the expression for the critical Froude number may differ somewhat from (10) for flow over a trough, it is still expected to be 0 (1), suggesting that nonlinear internal hydraulic phenomena may develop within the canyon, particularly during periods of stronger than normal flow.

We now compare our near field results with those obtained in previous canyon studies. Mayer *et al.* [1982] have reported a somewhat similar flow pattern to that in Figure 4 for the Hudson Shelf Valley: that is, for upstream conditions such that a mean flow is directed along isobaths perpendicular to the valley axis with shallow water to the right, seaward flow is observed in the valley. Our flow pattern is similar in that seaward flow occurs on the downstream side. Mayer *et al.* did not discuss the possible role of inertial boundary layers, but they were able to reproduce the down-valley flow using the Hsueh and Peng [1978] vorticity tendency equation which, for the barotropic case investigated by Mayer *et al.* [1982], takes the form

$$u_g H_x + v_g H_y = \frac{1}{\rho f} (\tau_{ox}^y - \tau_{oy}^x) \quad (11)$$

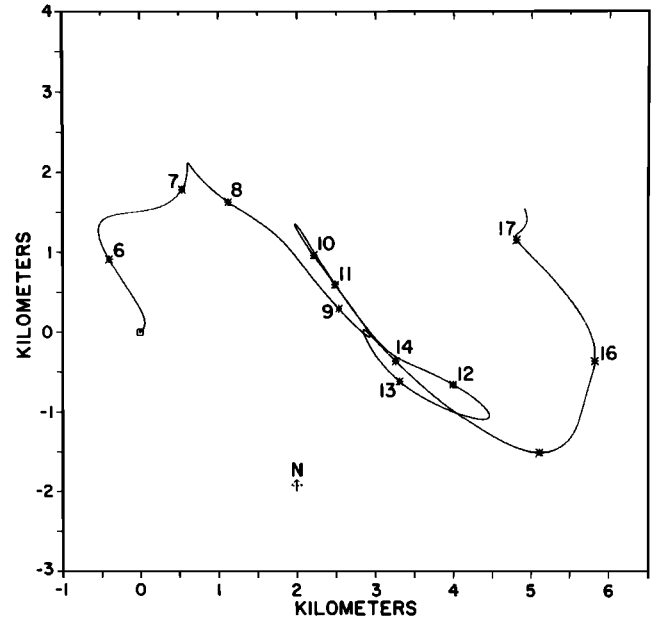


Fig. 13. Progressive vector diagram for the central axis lower current meter in 1981.

Here (u_g, v_g) are the geostrophic velocity components in the x and y directions, which are taken here to be positive on shelf and positive along shelf, respectively, as before. Equation (11) is linear and represents the cross-isobath flow induced by the curl of the bottom stress, which our measurements indicate is less important than advection of relative vorticity at Carson Canyon. It is readily obtained by taking the curl of the vertically integrated linearized shallow-water equations [e.g., Csady, 1982, p. 187], or from (4) by making the small Rossby number approximation. Using a linear bottom stress law ($\tau_o^x = \rho r u_g, \tau_o^y = \rho r v_g$), (11) takes the form

$$u_g H_x + v_g H_y = \frac{r}{f} (v_{gx} - u_{gy}) \quad (12)$$

If u_g and v_g are expressed in terms of the sea surface elevation, then (12) becomes identical to that used by Mayer *et al.* In the vicinity of the Hudson Shelf Valley, which is much longer than it is wide, cross-shelf (along-valley) gradients may be taken to be much smaller than along-shelf (cross-valley) gradients, and (12) becomes

$$u_{gy} = -\frac{fv_g}{r} H_y \quad (13)$$

As discussed by Mayer *et al.*, this implies that u_{gy} is negative on the upstream side of the valley where $H_y > 0$, and the flow therefore veers to the left. For the Hudson Shelf Valley the effect is large enough to produce downvalley flow over the valley axis for the upstream flow speeds considered. Carson Canyon is not very much longer than it is wide, however, and as a result, differences from the balance implied by (3), in addition to those arising from the assumption of linearity, should be expected.

4.3. Deep Flow in the Canyon

The residual currents registered by the instrument at 703-m depth on the central axis mooring are presented in Figure 13 in the form of a progressive vector diagram. The speeds are

weak, being 1 to 2 cm s⁻¹. During the 1981 upwelling event (June 8–15), the current is aligned with the canyon axis and oscillates between the upcanyon and downcanyon direction (Figure 4), with an approximate period of 2 days. Prior and subsequent to the event the residual current is directed roughly in the direction of the secondary head on the north-east side of the Canyon.

There have been two publications in which the residual flow within canyons affected by a strong cross-canyon flow above the canyon is discussed: Mayer *et al.* [1982], with respect to the Hudson Shelf Valley, and Freeland and Denman [1982], with respect to a spur canyon which is part of Juan de Fuca Canyon and is comparable in size to Carson Canyon. In both papers, headward flow deep within the canyon or shelf valley is investigated, but quite different mechanisms are invoked in each case.

Mayer *et al.* were able to show that the pressure gradient due to the cross-shelf sea surface slope associated with the long-term averaged flow on the shelf is reduced to zero by the opposing pressure gradient associated with the mean density field, at a depth above the level of intersection of the valley with the surrounding shelf. Within the canyon the densimetric pressure gradient apparently exceeds that due to the sea surface slope and, balanced by friction, drives a mean flow toward the head.

Freeland and Denman considered a case in which the mean geostrophic flow on the shelf is directed with shallow water to the left, the mirror image of the Carson Canyon situation, causing isopycnals on the slope to tilt upward toward the shelf. Within the canyon the pressure gradient associated with the geostrophic flow was assumed to be nonzero and could therefore drive a headward flow. The mass conservation equation was assumed to reduce to $\mathbf{u} \cdot \nabla \rho = 0$; that is, the flow is along isopycnals.

It is instructive to compare these situations with the Carson Canyon case. Because the Labrador Current extends to depths of about 200 m, the pressure gradient at the depth of the lower meter on the central axis mooring is probably controlled by the density field below the Labrador Current, and the observed headward motion at this depth could be explained by a mechanism similar to that invoked by Mayer *et al.* In the upper part of the canyon, however, the sea surface pressure gradient must be larger than the densimetric pressure gradient, as assumed by Freeland and Denman. Because the Labrador Current is directed with shallow water to the right, a pressure-gradient-driven flow of the type considered by Freeland and Denman would necessarily be directed out of the canyon. If this motion were also nondiffusive, then the flow would be directed upward and seaward from the canyon along isopycnals (Figure 2) over that depth range for which the pressure gradient associated with the geostrophic flow was nonzero. In addition, the Ekman transport in the bottom boundary layer on the shelf should be directed off shelf and into the canyon, possibly feeding the seaward along-isopycnal flow further downcanyon. This contrasts with the situation in the Juan de Fuca system and serves to illustrate the fundamental sidedness of the interaction of nearly geostrophic and baroclinic mean flows with canyonlike topographic features.

5. SUMMARY AND CONCLUSIONS

We have presented CTD and moored current meter measurements obtained in the vicinity of a submarine canyon

at the edge of the Grand Bank of Newfoundland. The data set contains a number of interesting and novel features.

In particular, an upwelling event of 6-day duration was observed. This event was characterized initially by abrupt temperature and salinity increases near the shelf break at the canyon perimeter and at shelf break depth over the canyon axis and occurred up to 1.5 days after the arrival of a storm in the region. Reversal or near-reversal of the mean flow was observed during this initial 1.5-day period. Reversal occurred later and was more prolonged over the canyon axis than at the shelf break instruments. Geostrophic velocity profiles indicate that reversal was confined to a zone of the order of 100 m thick spanning shelf break depth, and in the overlying water it was accompanied by a reduction in the local speed of the Labrador Current. It is argued that the reversal in the near-bottom zone at the shelf break is the result of a barotropic response directed opposite to the Labrador Current and induced by the upwelling favorable wind. The time scale associated with the canyon topography is estimated to be about 12 hours, suggesting that local effects are important in determining the nature of the response during the initial part of the event (i.e., at times less than about a day after onset). The duration of the event (6 days) is such, however, that friction and nonlocally generated disturbances, probably propagating from the upstream direction, undoubtedly become important.

The mean flow is characterized by approximate along-isobath flow in the far field upstream and downstream of the canyon. In the near field the flow is cross isobath and into the canyon on the upstream side, cross canyon at the canyon axis, and out of the canyon and somewhat shelfward of the along-isobath direction on the downstream side. Examination of the nonlinear and Coriolis acceleration terms in the momentum balance using the measured mean currents indicates that the nonlinear term involving advection of downstream momentum is important.

In order to investigate the topographic modification of the mean flow by the canyon, the stratification is idealized by a two-layer system, with the lower layer at rest. The flow shelfward of the 200-m isobath is taken to be barotropic and analyzed in terms of a vorticity tendency equation. The flow field is divided into near and far regions, the far field being defined as the region beyond the inertial boundary layer on the upstream side of the canyon. In the far field the equations of motion are approximately linear, and the vorticity tendency equation reduces to a form similar to that used by Hsueh and Peng [1978]: that is, Ekman pumping due to the curl of the bottom stress forces cross-isobath flow in the interior. If along-shelf variations are neglected, the sign of the mean shear of the Labrador Current at the shelf break is such that on-shelf motion is predicted. The associated on-shelf volume flux is estimated to be about 60 m³ s⁻¹ per 100 m of along-shelf distance, which is roughly the same as the on-shelf volume flux estimated from drifter tracks by Petrie and Isenor [1985]. This flux is large enough to importantly affect the balances of scalar quantities on the shelf and may be part of the explanation for the relatively infrequent observation of icebergs seaward of the shelf. This exchange mechanism has not to our knowledge been previously proposed for the Grand Bank and deserves further attention.

In the near field the Rossby number is not small, and the vorticity tendency equation represents a balance between advection of relative vorticity, vortex stretching by cross-isobath

flow, and bottom torque. Inertial effects appear to dominate friction and require that on the upstream side the Labrador Current cut across isobaths and flow into the canyon as observed. The flow in the near field is analyzed in the context of previous work on flow over bumps and flow in the atmosphere over mountain ridges, with the cross-stream depth gradient playing the role of the planetary vorticity gradient. It is found that this model is consistent at least qualitatively with most of the observations, including shelfward veering in the inertial boundary layer upstream, cross-isobath flow into deeper (shallower) water at the upstream (downstream) canyon wall, the deflection of dynamic height contours over the canyon axis, and the depression of isotherms and isohalines near the head of the canyon. Discrepancies between the observations and the model are attributed to the asymmetries in the canyon bathymetry, the nonzero relative vorticity in the far field, and the effects of stratification.

The circulation deep within the canyon induced by the mean flow above the canyon was investigated using models developed by Mayer *et al.* [1982] and Freeland and Denman [1982]. Both models produce headward flow but by quite different mechanisms. It appears that the circulation within Carson Canyon may share some features of each, but with an important difference which illustrates one aspect of the fundamental sidedness of the mean flow-canyon interaction problem. If the sea surface pressure gradient is not balanced or exceeded by the densimetric pressure gradient within the canyon, then Freeland and Denman assume that the residual drives a frictionless, nondiffusive flow which is necessarily along isopycnals. In their case (exterior geostrophic flow directed with shallow water to the left), this flow within the canyon was directed upward and on shelf. In the Carson Canyon case, because the Labrador Current flows with shallow water to the right, the same dynamics imply that a zone exists at intermediate depths within the canyon in which the flow is directed upward and off shelf, along isopycnal surfaces.

APPENDIX: EFFECTS OF FRICTION ON THE CURRENT MEASUREMENTS

These experiments were designed to monitor the upwelling of deep water onto the shelf. The current meters were therefore deployed as close to the bottom as possible. The penalty for this is that the measured velocities may have been affected by bottom friction. We now examine the probable magnitude of these effects.

Over a horizontal bottom in the unstratified case, the velocity defect thickness of the bottom boundary layer is given by [Caldwell *et al.*, 1972]

$$h_v \approx 0.4u_* / f \quad (\text{A1})$$

where u_* is the friction velocity. In the presence of stratification, Weatherly and Martin [1978] have suggested the following relation for the mixed layer thickness over a horizontal bottom:

$$h_m = 1.3 \frac{u_*}{f} \left(1 + \frac{N_0^2}{f^2} \right)^{-1/4} \quad (\text{A2})$$

where N_0 is the buoyancy frequency ($N_0^2 = -(g\partial\rho/\rho\partial z)$). Over a sloping bottom of infinite extent, however, with the interior geostrophic flow along isobaths with shallow water to the right, the mixed layer thickness increases with time, and the stable density difference at the top of the mixed layer

decreases due to downslope advection of less dense water within the boundary layer. We assume that in actual practice, growth would not continue indefinitely but would have the effect of increasing the vertical scale until cross-stream gradients, which were not considered in the model, would come into play.

The present situation is similar. The interior geostrophic flow is directed parallel to the isobaths with shallow water to the right. In the vicinity of the current meters, however, N_0^2 is small, about $6 \times 10^{-8} \text{ s}^{-2}$ (Figure 2f), and (A2) gives $h_m = 0.8 u_* / f$. This is twice the velocity defect thickness in the absence of stratification (equation (A1)), and given the above discussion, leads us to assume that the stratification is too weak to affect the velocity profile significantly.

Given (A1) and the additional relationship [Csanady, 1967; Armi and Millard, 1976]

$$u_* = (0.03 - 0.05)u_g \quad (\text{A3})$$

where u_g is the interior geostrophic speed, an estimate of u_* will yield estimates of both h_v and u_g , and the latter can be compared to the measured currents. We use the Kazanskii-Monin law [Kazanskii and Monin, 1961; Csanady, 1967]

$$\left(\frac{u_g^2}{u_*^2} - \hat{A}^2 \right)^{1/2} = \frac{1}{\kappa} \ln \frac{u_*}{fz_0} + \hat{B} \quad (\text{A4})$$

where z_0 is the bottom roughness parameter, $\kappa = 0.41$ is von Karman's constant, and \hat{A} and \hat{B} are constants. We also use the bottom boundary layer data collected by Weatherly [1972] as a guide, since the measured mean speed u_g (10 cm s^{-1}) and height above bottom (14 m) are comparable to ours, and in Weatherly's data the tidal current amplitudes were comparable to the mean speed. Weatherly found that $u_* = 0.04 u_g$, and this is the relationship used here (see equation (A3)). The constants \hat{A} and \hat{B} are assigned the values 19 and -4.1 , respectively. These are the values suggested by Kazanskii and Monin, satisfy (A4) with Weatherly's data ($u_* = 0.4 \text{ cm s}^{-1}$, $z_0 = 0.03 \text{ cm}$), and reproduce Weatherly's measured total veering (10°). Finally, we use

$$u_*^2 = C_D u_1^2 \quad (\text{A5})$$

where u_1 is the speed 1 m above bottom and C_D is the bottom drag coefficient, and the law of the wall

$$u = \frac{u_*}{\kappa} \ln \frac{z}{z_0} \quad (\text{A6})$$

From (A5) and (A6),

$$-\ln z_0 = \frac{\kappa}{(C_D)^{1/2}} \quad (\text{A7})$$

(z_0 in meters) and (A4) becomes

$$\left(\frac{u_g^2}{u_*^2} - \hat{A}^2 \right)^{1/2} = \frac{1}{\kappa} \ln \frac{u_*}{f} + \frac{1}{(C_D)^{1/2}} + \hat{B} \quad (\text{A8})$$

Sternberg [1968] has presented empirically determined drag coefficients for flow in tidal channels. A typical mean value is $C_D = 3 \times 10^{-3}$ and is the value assumed here. The reader is cautioned that since the ratio u_*^2/u_g^2 in (A8) is a drag coefficient referenced to the interior geostrophic speed rather than u_1 , the value of C_D should not be chosen independently of u_g/u_* . However, since Weatherly's data for u_g/u_* and u_*/f , when substituted in (A8), yield $C_D = 2.9 \times 10^{-3}$, our choice of

$C_D = 3 \times 10^{-3}$ is consistent with his measurements and therefore with $u_* = 0.04 u_g$. Substituting these latter values for C_D and u_g/u_* in (A8) gives $u_*f = 72$ m or, for $f = 10^{-4} \text{ s}^{-1}$, $h_b = 29$ m and $u_g = 18.1 \text{ cm s}^{-1}$. This value of u_g is comparable to the 1980 measured mean speeds. The value of h_b is typical of reported values for the ocean.

With $h_b = 29$ m, it is clear that the current meters were well within the boundary layer. The question remains as to what degree the measurements are expected to differ from the interior flow. Caldwell *et al.* [1972] took h_b to be the height at which $u = 0.99 u_g$. Examination of their Figures 20 and 21 indicates that the velocity profile changes slowly with height in the outer part of the boundary layer. Specifically, the velocity in the direction of the bottom stress equals the component of the interior geostrophic flow in this direction at a mean height of $(0.09 \pm 0.03)u_*f$, and at this height the mean speed is $(0.93 \pm 0.03)u_g$ and mean veering $6.6^\circ \pm 2.6^\circ$ to the left of u_g . Weatherly and Martin's [1978] numerical experiment for a horizontal bottom and unstratified fluid yields a similar result: from their Figure 6 at a height of $0.09 u_*f$, $u = 0.93 u_g$ and the veering angle is about 8.5° . Using (A1), this indicates that for distances above bottom greater than $0.23 h_b$, the mean speed will be within 10% of u_g , and the total leftward veering will be less than about 9° or 10° . In our case, with $h_b = 29$ m, this level is 6.6 m, and we conclude that the measured mean velocities at 8- and 10-m height probably differ by less than 10% in speed, and perhaps as little as 5° in terms of direction, from the interior geostrophic velocity. Since these differences are of the same order as the achievable accuracies reported for the instrument, we do not consider them to be significant.

Acknowledgments. We thank B. de Young, J. Foley, and A. Walsh for assistance in the field. We also thank the Captains and crews of MV *Pandora II* and *Gadus Atlantica*. Finally, we thank R. Greatbatch, for referring us to Holton's analysis and for enlightening discussions of the inertial boundary layer problem, and I. Webster, for valuable criticism of this manuscript. This project was funded by the Natural Sciences and Engineering Research Council, Canada, and the Department of Fisheries and Oceans, Canada. NICOS Contribution 102.

REFERENCES

- Armi, L., and R. C. Millard, Jr., The bottom boundary layer of the deep ocean, *J. Geophys. Res.*, **81**, 4983–4990, 1976.
- Bennett, A., Conversion of in situ measurements of conductivity to salinity, *Deep Sea Res.*, **23A**, 157–165, 1976.
- Bakun, A., Daily and weekly upwelling indices, west coast of North America, 1967–73, *NOAA Tech. Rep., NMFS SSRF-693*, 114 pp., Natl. Oceanic and Atmos. Admin., Seattle, Wash., 1975.
- Caldwell, D. R., C. W. Van Atta, and K. N. Helland, A laboratory study of the turbulent Ekman layer, *Geophys. Astrophys. Fluid Dyn.*, **3**, 125–160, 1972.
- Coachman, L. K., and C. A. Barnes, Surface water in the Eurasian Basin of the Arctic Ocean, *Arctic*, **15**, 251–277, 1962.
- Csanady, G. T., On the "resistance law" of a turbulent Ekman layer, *J. Atmos. Sci.*, **24**, 467–471, 1967.
- Csanady, G. T., *Circulation in the Coastal Ocean*, 279 pp., D. Reidel, Hingham, Mass., 1982.
- Freeland, H. J., and K. L. Denman, A topographically controlled upwelling center off southern Vancouver Island, *J. Mar. Res.*, **40**, 1069–1093, 1982.
- Gill, A. E., *Atmosphere-Ocean Dynamics*, 662 pp., Academic, Orlando, Fla., 1982.

- Godin, G., *The Analysis of Tides*, 264 pp., University of Toronto Press, Toronto, Canada, 1972.
- Hay, A. E., and E. D. Kinsella, Steady wind-driven upwelling in the presence of a baroclinic coastally trapped jet, *J. Phys. Oceanogr.*, **16**, 1359–1369, 1986.
- Hogg, N. G., Effects of bottom topography on ocean currents, *GARP Publ. Ser.*, **23**, 167–205, 1980.
- Holton, J. R., *An Introduction to Dynamic Meteorology*, 391 pp., Academic, Orlando, Fla., 1979.
- Hotchkiss, F. S., and C. Wunsch, Internal waves in Hudson Canyon with possible geological applications, *Deep Sea Res.*, **29**, 415–442, 1982.
- Hsueh, Y., and C. Y. Peng, A diagnostic model of continental shelf circulation, *J. Geophys. Res.*, **83**, 3033–3041, 1978.
- Huthnance, J. M., Waves and currents near the continental shelf edge, *Prog. Oceanogr.*, **10**, 193–226, 1981.
- Inman, D. L., C. E. Nordstrom, and R. E. Flick, Currents in submarine canyons: An air-sea-land interaction, *Annu. Rev. Fluid Mech.*, **8**, 275–310, 1976.
- Kazanskii, A. B., and A. S. Monin, On the dynamic interaction between the atmosphere and earth's surface, *Izv. Akad. Nauk SSSR Ser. Geofiz.*, **5**, 786–788, 1961.
- Kinsella, E. D., Wind and topographic effects on the Labrador Current at Carson Canyon, 195 pp., M. Sc. thesis, Mem. Univ. of Newfoundland, 1984.
- Long, R. R., Some aspects of the flow of stratified fluids, I, A theoretical investigation, *Tellus*, **5**, 42–57, 1953.
- Mayer, D. A., H. O. Mofjeld, and K. D. Leeman, Near-inertial interval waves observed on the outer shelf in the Middle Atlantic Bight in the wake of hurricane Belle, *J. Phys. Oceanogr.*, **11**, 87–106, 1981.
- Mayer, D. A., G. C. Han, and D. V. Hansen, Circulation in the Hudson Shelf Valley: MESA physical oceanographic studies in New York Bight, **1**, *J. Geophys. Res.*, **87**, 9563–9578, 1982.
- Mountain, D. G., Direct measurements in the Labrador Current, *J. Geophys. Res.*, **85**, 4097–4100, 1980.
- Pedlosky, J., *Geophysical Fluid Dynamics*, 624 pp., Springer-Verlag, New York, 1979.
- Petrie, B., Current response at the shelf break to transient wind forcing, *J. Geophys. Res.*, **88**, 9567–9578, 1983.
- Petrie, B., and C. Anderson, Circulation on the Newfoundland Continental Shelf, *Atmos. Ocean*, **21**, 207–226, 1983.
- Petrie, B., and A. Isenor, Near-surface circulation and exchange in the Newfoundland Grand Banks region, *Atmos. Ocean*, **23**, 209–227, 1985.
- Shaffer, G., A mesoscale study of coastal upwelling variability off NW Africa, *Meteor. Forschungsergeb., Reihe A*, **17**, 21–72, 1976.
- Shepard, F. P., N. F. Marshall, P. A. McLoughlin, and G. G. Sullivan, Currents in submarine canyons and other seavalleys, *AAPG Stud. Geol.*, no. 8, 173 pp., 1979.
- Sternberg, R. W., Friction factors in tidal channels with differing bed roughness, *Mar. Geol.*, **6**, 243–260, 1968.
- Weatherly, G. L., A study of the bottom boundary layer of the Florida Current, *J. Geophys. Res.*, **2**, 54–71, 1972.
- Weatherly, G. L., and P. J. Martin, On the structure and dynamics of the oceanic bottom boundary layer, *J. Phys. Oceanogr.*, **8**, 557–570, 1978.

W. W. Denner, Science Applications International Corporation, Monterey, CA 93905.

Alex E. Hay, Department of Physics and Newfoundland Institute for Cold Ocean Science, Memorial University of Newfoundland, St. Johns, Newfoundland, Canada A1B 3X7.

E. Douglas Kinsella, WASC Oceanographic Services Department, Edgerton, Germeshausen, and Grier, Incorporated, Waltham, MA 02154.

(Received November 24, 1986;
accepted January 13, 1987.)